Moroccan Journal of Chemistry
ISSN: 2351-812X
http://revues.imist.ma/?journal=morjchem&page=login
K. Toumiat / Mor. J. Chem. 4N°4 (2016) 1144-1156

Electrochemical, Chemical and Theoretical Studies of Copper Corrosion Inhibition using Iodate Ions from Potassium Iodate as an Inorganic Inhibitor in 0.5 M NaCl Solution

K. Toumiat [(a)*], ***A. Guibadj*** [(a)]

[(a)] *laboratory of Physical Chemistry Materials, Laghouat University, Algeria*

Abstract

The present work aims to test the inhibition effect of iodate ions present in potassium iodate, as an inorganic inhibitor for copper corrosion in sodium chloride medium. Chemical and electrochemical methods are carrying out such as weight loss, potentiodynamic and Electrochemical Impedance Spectroscopy (EIS). The present study confirm that the IO_3^- acts as a mixed type inhibitor for copper in 0.5 M NaCl. The iodate ions shows an important inhibition efficiency with 20 ppm for copper in sodium chloride medium. The surface characterization performed using Scanning Electron Microscopy (SEM) method to confirm the adsorption of the inhibitor molecules on copper surface after an immersion of 16 days in aerated 0.5 M NaCl. Computer simulation confirm that the IO_3^- molecules adsorbed on Cu (110) surface. Technics used in this research are in very good agreement and revealed that the IO_3^- is a good inhibitor for copper corrosion in sodium chloride medium.

* *Corresponding author:* k.toumiat@lagh-univ.dz

Received 28 Sept 2016,
Revised 05 Dec 2016,
Accepted 16 Jan 2017

Keywords: *Copper, corrosion inhibition, weight loss, computational details, IO_3^-.*

1. Introduction

From a wide range of metals used in industries, copper extensively used owing to its remarkable thermic and electric properties. It is usually employed in heating and cooling systems because of its excellent thermal conductivity [1- 7]. Copper also exclusively used for piping and delivery of water in marine industry. These pipes used in a medium rich of [8]. It is known that the corrosion products caused by chloride ions leads to a reduction in the efficiency of copper, which causes huge economic loss [9, 10]. The corrosion inhibition is one of several methods of protection against metals degradation in different aqueous solutions [11-15]. The use of inorganic inhibitors as an alternative to the organic inhibitors based on the possibility of its degradation with time and temperature [16]. To prevent the problem of corrosion, it is very important to add corrosion inhibitors. From several ways of corrosion inhibition, the use of oxidizing agents like IO_3^- into a corrosive medium, can lead to self-passivation of copper. Other studies also reported that the iodate react as an effective inhibitor for copper in acidic environments. The IO_3^- behaves as an oxidizer at low concentrations and as a passive agent with higher concentrations for copper dissolution, with a strong adsorption of these ions on copper surface forming [17]. Iodate processes remarkable corrosion inhibition, anti-microbial and oxidizing properties. Until now, no research had been publishes on the use of IO_3^- as inhibitor for copper in NaCl medium. To overcome this problem, an electrochemical monitoring done by studying the behavior of copper in 0.5 M NaCl in presence and absence of the iodate inhibitor.

2. Materials and methods

2.1. Chemicals and preparation of samples

KIO_3 (Fluka, 99.5 %), NaCl (0.5 M) electrolyte prepared using deionized water, a three electrodes electrochemical cell was used which contains: counter electrode of platinum (Pt: 1cm²) and Saturated Calomel Electrode (SCE). As reference electrode. The working electrodes were made using pure copper 99.99% cylinder; the samples were mechanically (D1= 1.1 cm, D2 = 0.8 cm) x 1 cm dimensions. The samples used for electrochemical study were welded with electrical cables for easier use, then coated with epoxy resin and finally polished with abrasive paper (1200, 1500, 2000 and 2500) followed by a finishing polishing (Felt) with diamond polishing paste (0.1µm). The samples used for weight loss experiment polished by the same way. All samples cleaned successively with acetone, distilled water then deionized water.

2.2. Electrochemical measurements

The potentiodynamic polarization and EIS measurements performed, using an Auto lab (PGZ-402) electrochemical workstation and an electrochemical cell (100 ml) with three electrodes, the solution was not stirred or deaerated. Before the potentiodynamic polarization measurements, an open circuit measurement for 30 min was performed to stabilize the potential. The potential was scanned from - 400 to 400 mV at a scan rate of 1mV.min-1. The EIS measurements were performed at open circuit potential for 30 min, in a frequency range from 100 KHz to 100 mHz.

2.3. Weight loss and SEM analyses

Samples used for weight loss measurement were preparing by the same method mentioned previously. In a cylindrical shape (d = 0.8 cm & h = 0.3 cm) with an exposed total area (A=1.76 cm²). After polishing and weighting (m_1) the Samples introduced in 100 ml 0.5 M of NaCl solution with and without inhibitor used for (2- 16) days. Subsequently, the tested samples were removed, cleaned and weighted (m_2). In order to see if the iodate molecules effectively adsorbed on the copper surface executed the SEM analysis, SEM is widely used to detect the morphological features

of metal surface. The SEM micrograph have obtained for copper samples used in weight loss part. The surface morphology of these copper samples investigated by using SEM analysis (VEGA 3, TESCAN) at 5, 10 and 20.0 KV.

2.4. Computational details

Molecular dynamics studies carried out using Materials Studio 7 software, from accelrys Inc. To find the correlation between theoretically calculated properties and experimentally determined inhibition efficiency for copper corrosion in 0.5 M NaCl solution by iodate as inorganic inhibitor. The DMol^3 semi-empirical tight binding method was used for building and optimize iodate molecule, determine the electronic properties of IO_3^-, effect of the frontier molecular orbital energies The energy of the highest occupied molecular orbital (E_{HOMO}), the energy of the unoccupied molecular orbital (E_{LUMO}), electronic charges on reactive centers, dipole moment and the energy of the gap Equation (1).

$$\Delta E = E_{LUMO} - E_{HOMO} \quad (1)$$

Interaction between iodate molecules and Cu (110) surface carried out in a simulating box (14.45 Å×10.22Å × 29.99 Å) with periodic boundary conditions. The Cu (110) surface was fist built and relaxed by minimizing its energy, using molecule mechanics then the surface of Cu (110) was increasing by constructing a supercell, a vacuum slab of 30 Å thickness built on the Cu (110) surface. The number of layers in the structure was chosen so that the depth of surface is greater than the non-bond cutoff used in the calculation; we choose 6 as a number of layers which sufficient depth that the inhibitor molecules will only be involved in non-bond interactions with Cu (110) surface. After minimizing Cu (110) surface and iodate molecules, the corrosion system will built by layer builder to place the inhibitor molecule on Cu (110) surface using a forcefield Universal. The adsorption locator module in Materials Studio 7 software from accelrys Inc. [19] allows selecting thermodynamic ensemble and associated parameters, temperature and pressuring and initiating a dynamic calculation. The dynamic simulations procedures have been described elsewhere [20].

3. Results and Discussions

3.1 Potentiodynamic Polarization results

Potentiodynamic polarization curves are showing in (Figure 1) represents the behavior of pure copper electrodes in aerated 0.5 M NaCl solution at room temperature, without and with 20 ppm of iodate after an immersion time of 30 min as open circuit potential measurement.

The cathodic corrosion reaction of copper in NaCl solution is the reaction of oxygen [21-24]:

$$O_2 + 2\,H_2O + 4\,e^- \rightarrow 4\,OH^- \quad (2)$$

Usually, the dissolution of copper (anodic corrosion reactions) is:

$$Cu \rightarrow Cu^+ + e^- \quad (3)$$

Moreover, Cu^+ ions can undergo disproportionation according to Equation (3) [21-24]

$$2Cu^+ \rightleftharpoons Cu^{2+} + Cu \quad (4)$$

When we use an aerated corrosive aqueous medium in near neutral pH, which contained complexing agents such as Cl^-, we have to consider the formation of copper complex such as $CuCl_2^-$; which the anodic reactions are as following:

$$CuCl_{ads} + Cl^- \rightleftharpoons CuCl_2^- \quad (5)$$

$$Cu + Cl^- \rightleftharpoons CuCl_{ads} + 1\,e^- \quad (6)$$

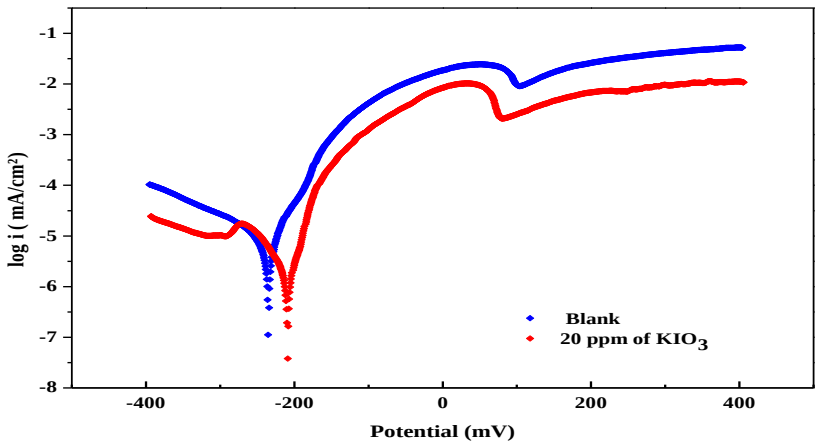

Figure 1: Polarization curves of copper electrode at an open-circuit potential after 30 min without and with 20 ppm of iodate in aerated 0.5 M NaCl solution.

Compared with the solution without inhibitor the corrosion potential (E_{corr}) displaced to the more positive values and both the anodic and cathodic currents (i_{corr}) were decreased. This indicates that the iodate inhibitor acts as a mixed-type corrosion inhibitor. The cathodic and the anodic currents progressively diminish by adding the iodate, which is clearer in anodic current. The results obtained using Tafel extrapolation method. In (Figure 1) it is clear that the cathodic polarization curves does not display an extensive Tafel region, which confirm a limiting diffusion current return to the reduction of dissolved Oxygen, the Tafel extrapolation method used for both anodic and cathodic Tafel region using Voltamaster 4.0 program. The kinetics of electron transfer at the metal-solution interface can be shown using Butler-Volmer equation [25]. For these study the Butler –Volmer equation given by Equation (7).

$$i=i_{corr}-\left[e^{\alpha nF\,(E-E_{corr})/RT}-e^{-(1-\alpha)\,nF\,(E-E_{corr}/RT)}\right] \qquad (7)$$

Where i_{corr} is the corrosion current density at the corrosion potential E_{corr}, α is the transfer coefficient (usually 0.5), and n the number of electrons transferred. When the rate of the back reaction is negligible, Equation (7) gives:

$$E=a+b\log i \qquad (8)$$

Where a and b constants. In Equation (8), when $E=E_{corr}$ and when $i=i_{corr}$ this is the basis of Tafel exploitation. The inhibition efficiency ($\eta i\,(\%)$) shown in Table 1 was calculated from values of (i_{corr}) using the following equation:

$$\eta i\,(\%)=\frac{i^{0}_{corr}-i_{corr}}{i^{0}_{corr}}\times 100 \qquad (9)$$

Where i^{0}_{corr} and i_{corr} are the corrosion current densities for Cu electrode in in aerated 0.5 M NaCl in absence and presence of iodate. The electrochemical parameters shown in (Table 1) extracted from polarization curves shown in (Figure 1) obtained after an electrochemical follow of the behavior of pure copper in 0.5 M NaCl medium in absence and presence of 20 ppm of KIO_3 at room temperature.

It can be conclude that the corrosion current density decreased and the inhibition efficiency increased with adding of iodate, which adsorbed on copper surface acted as a barrier layer to block corrosion process. Addition of 20 ppm of iodate reduces to good importance. With an inhibition efficiency, 72.16% obtained for 20 ppm of iodate. To overcome this problem, an electrochemical monitoring done by studying the behavior of copper in 0.5 M NaCl in presence and absence of the iodate inhibitor.

Table 1: Corrosion inhibition parameters of copper in aerated 0.5 M NaCl solution in the absence and presence of IO_3^-

C (ppm)	E_{corr} (mV/SCE)	Rp (KΩ/cm²)	b_a ($mV.dec^{-1}$)	b_c (mV.dec-1)	i_{corr} (µA.cm-²)	ηi (%)
Blank	-233.9	1.49	47.0	-152.9	9.7	--
20 ppm IO_3^-	-153.1	3.69	27.3	-198.2	2.7	**72.16**

3.2 EIS results

In this experimental part of electrochemical measurements, the Electrochemical Impedance Spectroscopy (EIS) used to confirm results of the potentiodynamic polarization step and to get further information of the inhibition process with the same concept with potentiodynamic measurement. The EIS is an excellent tool to investigate the corrosion and the adsorption phenomena. [25]. Several experiences were done using copper electrode in different electrolytes without and with the inhibitor (IO_3^-) in aerated 0.5 M NaCl medium at room temperature. The results obtained at an open circuit potential immersed for 30 min represented as typical Nyquist and Bode plots, shown in (Figures 2, 3 and 4).

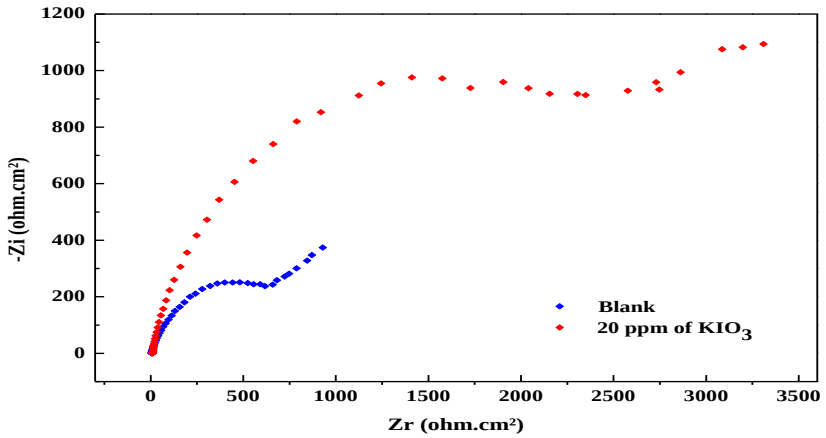

Figure 2: Nyquist plots of copper electrode at an open-circuit potential after 30 min without and with 20 ppm of IO_3^- in aerated 0.5 M NaCl solution.

In the presence of IO_3^- the impedance spectra for the Nyquist plots (Figure 2) shows a depressed semicircle in the high frequency region. This high frequency semicircle attributes to the charge transfer and double layer capacitance [26]. The lowest frequency area which generally known as Warburg impedance related to the diffusion of soluble copper species from electrode surface to bulk solution [26]. The diameter of semicircles in extent in the presence of the inhibitor. The Bode plots (Figure 3) show that the impedance values over the whole frequency range increased in the presence of IO_3^-.

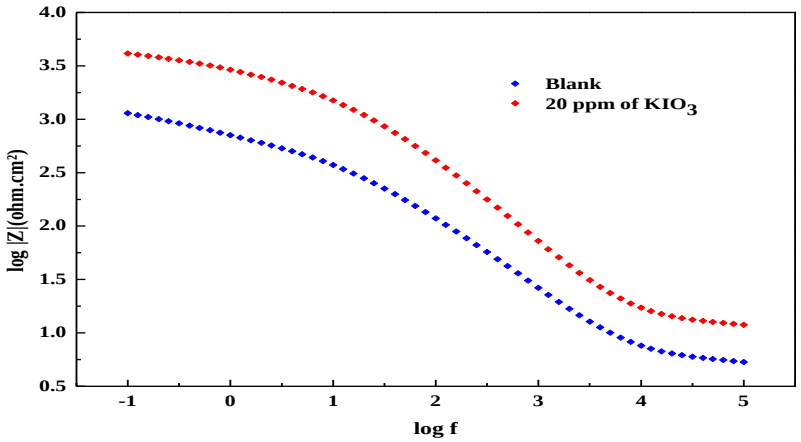

Figure 3: Bode plot for copper electrode without and with 20 ppm of IO_3^- in aerated 0.5 M NaCl solution.

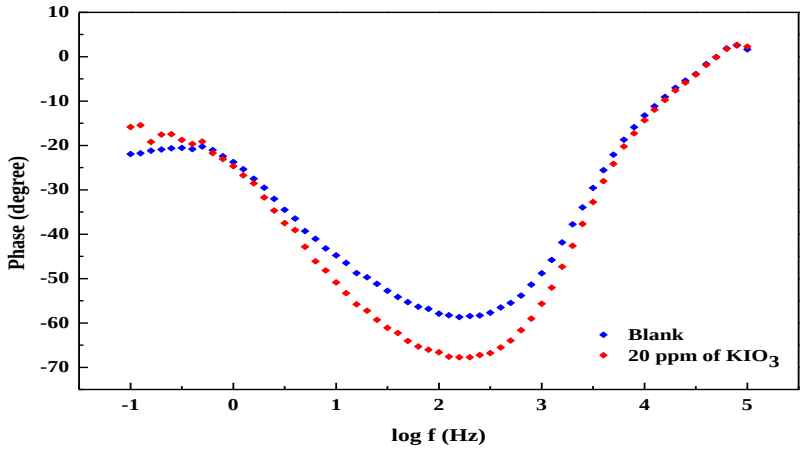

Figure 4: Phase angle plot for copper electrode without and with 20 ppm of IO_3^- in aerated 0.5 M NaCl solution.

It can be obtains from Bode phase plots (Figure 4) that the corrosion process-taking place at the electrode surface has one relaxation time constant related to the relaxation of the electrical double layer capacitor. It is also observed that the presence of iodate increase the maximum phase angle which confirm the inhibiting action of IO_3^- on copper in the study medium. The equivalent circuit model illustrated in Figure 5 is used to construe impedance characteristics is shown in this circuit was reported in several studies for copper/solution interface [26, 27].

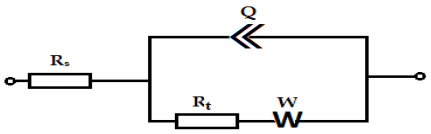

Figure 5: Equivalent circuit used to fit experimental EIS data in Figure3 (symbols in the circuit indicated in the text).

The parameters obtained by fitting the equivalent circuit and the inhibition efficiency represented in Table 2. Here R_s represents the solution resistance; Q represents the constant phase element (CPE); R_t represents the charge transfer resistances; and W is the Warburg impedance. The impedance of CPE represented by the following equation:

$$Q=Y_0(j\omega)^n \qquad (10)$$

Where Y_0 is the modulus, j is the imaginary root, **ω** is the angular frequency and n is the phase.

In the practical electrode system, the impedance spectra are offer depressed semicircles with their centres below the real axis. This phenomenon known as the dispersing effect [28]. The inhibition efficiency (η_i) is calculated using charge transfer resistance as follow:

$$\eta_i = \left(1 - \frac{R_{t_0}}{R_t}\right) \times 100 \qquad (11)$$

Table 2: Impedance parameters for copper electrode without and with 20 ppm of IO_3^- in aerated 0.5 M NaCl solution.

Solution	Parameters					
	$R_S(\Omega)$	Q $Y_0(\mu F.s^{a-1})$	a	$R_t(\Omega)$	W ($\Omega.s^{-1/2}$)	η_i (%)
Blank	11.43	66.27	0.920	797.6	784.9	--
20 ppm of IO_3^-	09.97	36.06	0.797	2 579	653.8	**69.07**

3.3 Weight loss and SEM analyses results

In this part the variation of the weight loss of copper at different immersion times in aerated 0.5 M NaCl solution, at room temperature 25°C for (2, 4, 7, 10, 14 and 16) days, without and with 20 ppm of IO_3^- results shown in (Figure 6).

The concentration of inhibitor used in this part was chosen as same as the concentration in the electrochemical study part. The loss of weight mentioned (Δm : $mg.cm^{-2}$).

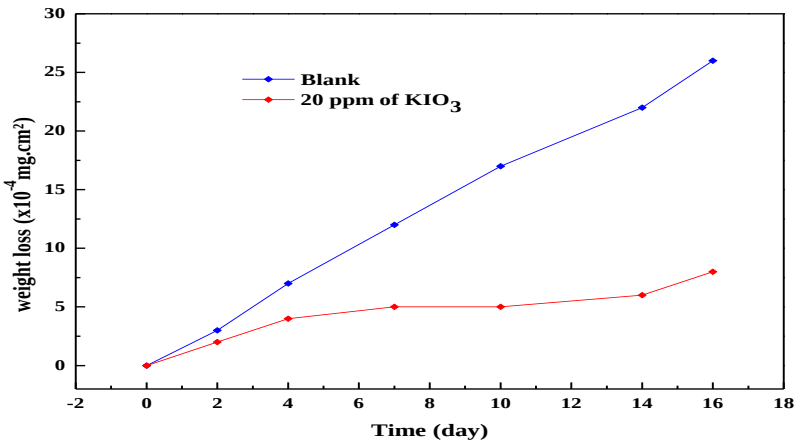

Figure 6: Variation of the weight loss with time of copper coupons in aerated 0.5 M NaCl solution without and with 20 ppm of IO_3^-.

The corrosion rate (R_{corr}) and the inhibition efficiency $\eta_w(\%)$ calculated as follow [29, 30]:

$$\Delta m = \frac{m_1 - m_2}{A} \qquad (12)$$

$$R_{corr} = \frac{\Delta m}{At} \qquad (13)$$

$$\eta_w(\%) = \frac{R_{corr}^{un} - R_{corr}^{in}}{R_{corr}^{un}} \qquad (14)$$

Here, A is the total area exposed to the solution; t is the time of immersion; R_{corr}^{un} is the corrosion rate without inhibitor; and R_{corr}^{in} is the corrosion rate with inhibitor. The inhibition efficiencies calculated in this part figured in the Figure 7,

it is clear that the iodate has a good effect against copper corrosion in the study medium; also, it stays effective after 16 days of immersion without forget the low concentration of inhibitor used in this part.

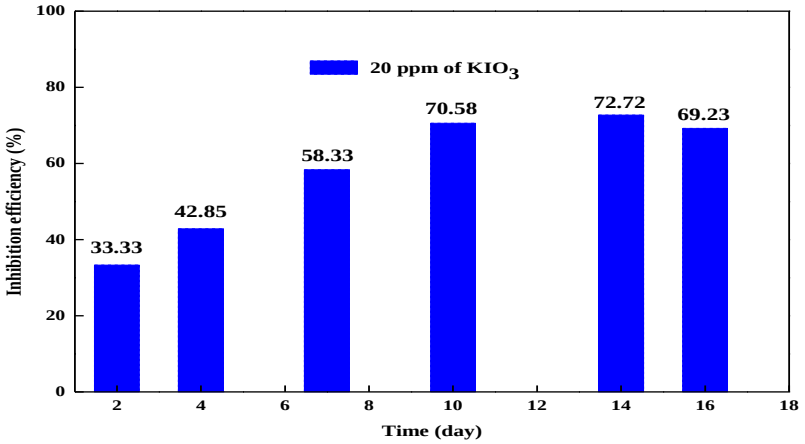

Figure 7: Variation of the inhibition efficiency with time of copper coupons in aerated 0.5 M NaCl solution without and with 20 ppm of IO_3^-.

The SEM micrograph for the copper samples immersed in aerated 0.5 M NaCl in absence and presence of iodate with concentration 20 ppm for 16 days shown in (Figures 9 (a) and (b)). It is obvious that the iodate molecules are partially distributing on the copper surface.

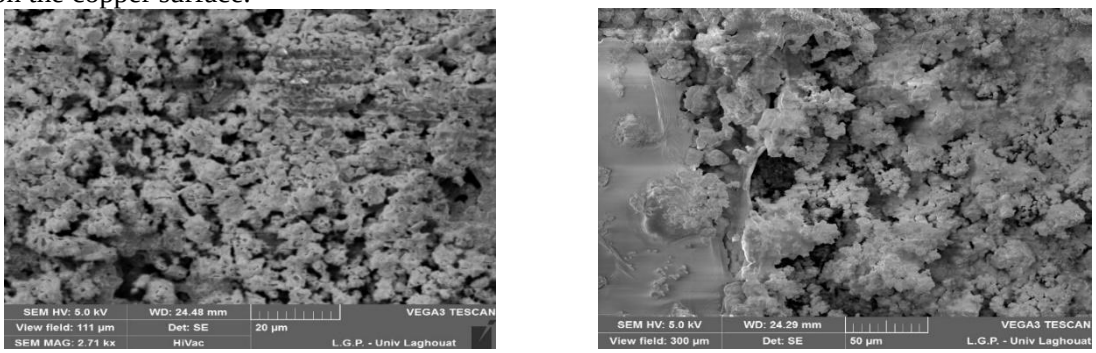

(a) **(b)**

Figure 8: SEM images for copper electrodes after 16 days immersion in aerated 0.5 M NaCl solution without inhibitor **(a)** and with 20 ppm of iodate **(b)**.

The surface coverages obtained from:

$$\theta = \frac{m - m_{inh}}{m} \qquad (15)$$

m, m_{inh} : are weight loss obtained from previous measurements. The corrosion rates obtained from Equation (15).

The inhibition efficiency, coverages and corrosion rates tabulates as follow:

The (Figure 8.a) represent the copper sample before immersion, the **(**Figure 8.b**)** shown the sample the surface morphology of copper sample immersed in solution without inhibitor, it is clear that surface strongly corroded by the Sodium Chloride solution. The last figure shows the morphology of the copper sample, immersed in the solution contains 20 ppm of iodate. Protection layers were formed on the copper surface, it can be concluded that the IO_3^- has a good inhibiting effect on copper corrosion which confirmed in weight loss part, at 20 ppm of iodate an after 16 days the inhibition efficiency attain 72.72 %.

Table 3: The inhibition efficiency $\eta_w(\%)$ changes of the degree of copper surface coverages (θ) and corrosion rates R_{corr}^{un} : without inhibitor and R_{corr}^{in} **:** with 20ppm of IO_3^-) obtained from weight loss data in aerated 0.5 M NaCl

20 ppm IO_3^-	**Time**					
	2 days	**4 days**	**7 days**	**10 days**	**14 days**	**16 days**
η_w **(%)**	33.33	42.85	58.33	70.58	72.72	69.23
θ **(10^{-4})**	1.35	2.71	3.39	3.39	4.06	5.42
R_{corr}^{un} **(10^{-5} cm/d)**	8.52	9.94	9.74	9.65	8.92	9.23
R_{corr}^{in} **(10^{-5} cm/d)**	5.68	5.68	4.05	2.84	2.43	2.84

3.4. Theoretical studies results

3.4.1. DMol^3 simulation results

The present part focus on the geometry optimization step of the iodate molecule using *DMol*^{3} module, this optimization step aim to calculate the Mullikan charge distributions of iodate as well as E_{HOMO} and E_{LUMO}), were calculated and represented in (Figure 9). It is found that the E_{HOMO} is located on the Oxygen atoms which indicate that the preferred active sites for an electronic attack and the favourite sites for interactions with the metal surface are located within the region around the Iodine (iodate IO_3^-) atoms.

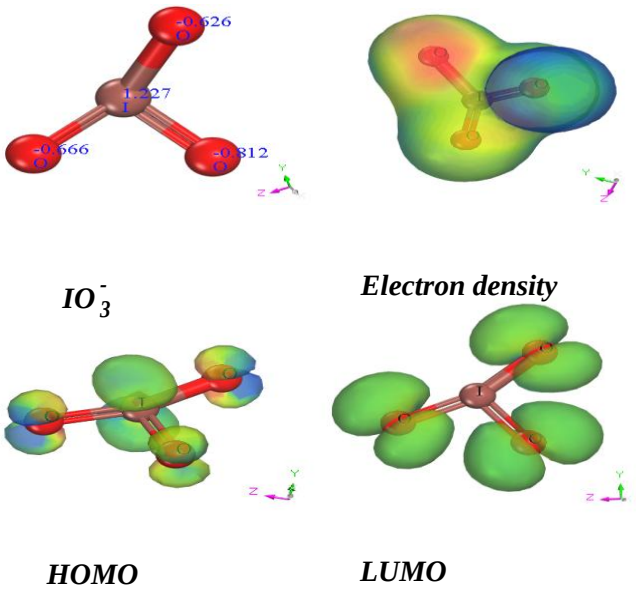

Figure 9: Charge distribution; Electron density; and frontier molecular orbitals for the optimized IO_3^- by DMol^3 module

According to DFT-Koopmans' theorem [32], the ionization potential *I* can be write as follow:

$$I=-E_{HOMO} \quad (16)$$

Then the negative of the energy of the LUMO represent the electron affinity *A* Equation (17):

$$A=-E_{LUMO} \quad (17)$$

Other quantum chemical parameters has been correlated recently using DFT modules [33], these calculated parameters such as dipole moment μ which given as follow:

$$\mu=qR \quad (18)$$

where q represents the charge and R is the distance.

The value of the electronegativity χ and the chemical potential [34] gives by Equation (19):

$$\chi=(I+A)/2 \quad (19)$$

Other parameters [35, 36] can be calculate such as the global hardness η and the global softness where the global hardness given by Equation (20):

$$\eta=(I+A)/2 \quad (20)$$

The global softness S or the absolute hardness is define by the inverse of the global hardness where:

$$S=1/2\eta \quad (21)$$

The propensity of chemical species to accept electrons is define as the global electrophilicity ω it was gives by Par et Al. [37] as follow:

$$\omega=\mu^2/4\eta \quad (22)$$

The Equation (22) can be write as follow:

$$\omega=\frac{(I+A)^2}{8(I+A)} \quad (23)$$

Obtained results for IO_3^- molecule and interaction of IO_3^- molecule with copper surface calculated with DMol^3 module showed in Table 4.

Table 4: Quantum chemical and molecular dynamics parameters for IO_3^- molecule calculated with DMol^3 module in aqueous phase

Propriety	***Value***
E_T, ***au***	-7736.522
μ, D	10.735
E_{HOMO}, ***eV***	-5.713
E_{LUMO}, ***eV***	-1.829
ΔE, ***eV***	3.884
I	5.713
A	1.829
X	3.771
η	1.942
S	0.257
ω	0.942

The high value of E_{HOMO} (-5.713 eV) indicate the tendency of IO_3^- molecule to donate electrons to the appropriate acceptor molecule with the low energy and the empty molecular orbital. Whereas the value of E_{LUMO} (-1.829 eV) indicate the ability of IO_3^- molecule to accept electrons. Observing the value of the energy of the gap ΔE which indicate the stability of the formed complex ($Cu\text{-}IO_3^-$).

3.4.2. Molecular dynamics simulation

Forcite tools, adsorption locator, molecular dynamics in Materials Studio 7 software from accelrys Inc. [20] performed on a system comprising IO_3^- molecule and Cu (110) surface. The IO_3^- molecule placed on the surface of copper, optimized then quench molecular dynamics run. (Figure 10) shows the optimization energy step for IO_3^- molecule, before putting it on the Cu (110) surface.

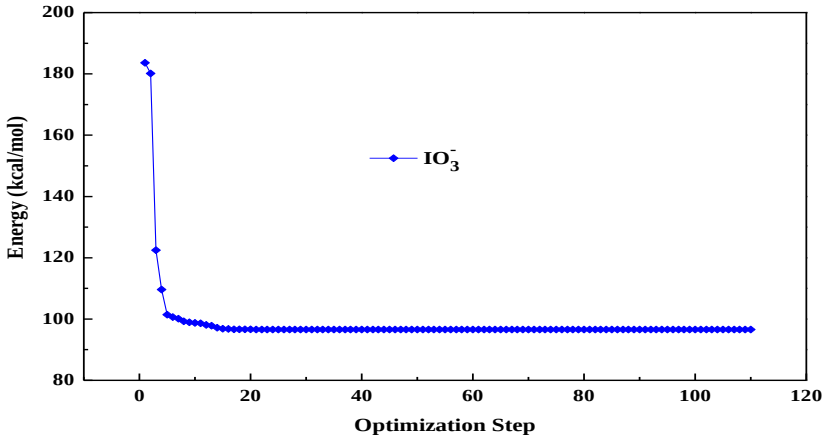

Figure 10: Geometry optimization energy step of IO_3^- using Forcite module.

Total energy, average energy, Van der Waals energy, electrostatic energy and intermolecular energy in interaction of $IO_3^-/Cu(110)$ surface figured in (Figure 11).

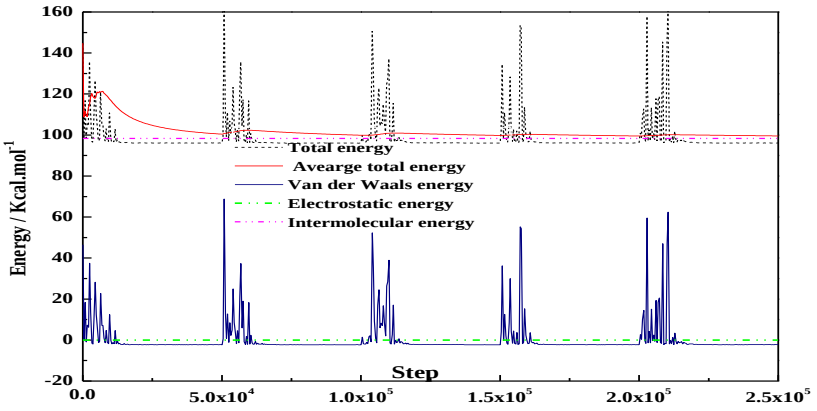

Figure 11: Total energy distribution for IO_3^-/Cu system during energy optimization process.

The adsorption locator process tries to get to the lowest energy for the system in comprising $IO_3^-/Cu(110)$. The possibility of IO_3^- adsorption on Cu (110) surface simulated in (Figure 12 (a)). We can see from (Figure 12 (b)) that iodate molecule moves near to the copper surface, indicating that the iodate adsorbed at copper surface. Figure 12(a) shows that the adsorption occurred through the Iodine atoms. The adsorption density of IO_3^- on Cu (110) surface shown in (Figure 12 (b)). Therefore, the studied molecules are likely to the copper surface to form a stable adsorption layer and protect copper from corrosion. The parameters tabulated in Table 5 include total energy of the $IO_3^-/Cu(110)$ configuration. The total energy is defined is the sum of the energies of the adsorbate components, the rigid adsorption energy and the deformation energy. In the present study, the energy of the substrate (Cu (110) surface) taken as zero.

Then adsorption energy reports energy required when the relaxed adsorbate iodate, adsorbed on the substrate surface Cu (110). The adsorption energy defined as the sum of rigid adsorption energy and the deformation energy for iodate molecule.

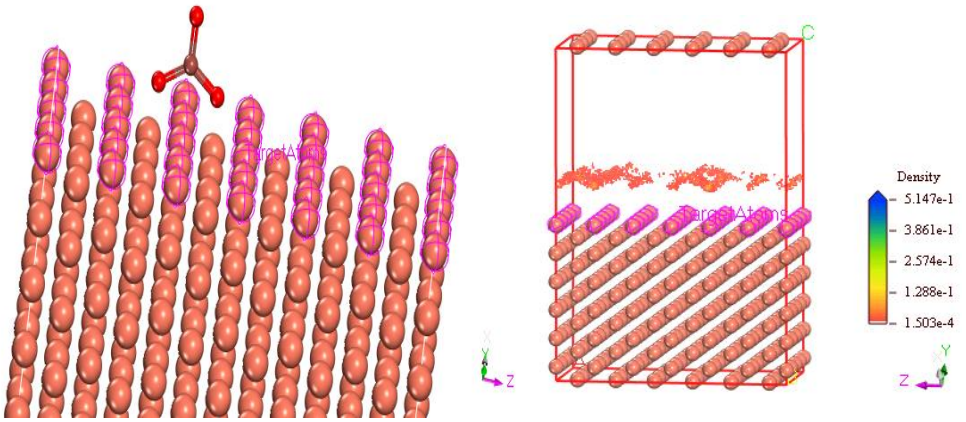

(a) **(b)**

Figure 12: (a) Most suitable configuration for adsorption of iodate on the Cu (110) surface obtained by Adsorption locator module; **(b)** Adsorption density of iodate on the Cu (110) substrate.

The rigid adsorption energy released when the unrelaxed iodate molecule (before geometry optimization step) adsorbed on Cu (110) surface. The deformation energy required when the iodate molecule is relaxed on the Cu (110) surface. The report (dE_{ads}/ dN_i) of IO_3^-/Cu(110) configurations where one of the iodate molecule has been removes also shown in Table 5.

Table 5: Outputs and descriptors calculated with adsorption locator for iodate on Cu (110) surface

Inhibitor	**IO_3^-**
Total energy (Kcl.mol^{-1})	94.48
Adsorption energy (Kcl.mol^{-1})	-3.84
Rigid adsorption energy (Kcl.mol^{-1})	-2.11
Deformation energy (Kcl.mol^{-1})	-1.72
dE_{ads}/ dN_i (Kcl.mol^{-1})	-3.84

4. Conclusion

The iodate known as a good inhibitor for several metals corrosion in aqueous solutions. In the present study, the inhibition mechanism is attributable to the adsorption of the inhibitor on the copper surface and blocking its active sites. Results obtained from electrochemical measurements Potentiodynamic polarization and EIS techniques and from chemical measurement, using weight loss method are reasonably in good accord. To go so far and follow the stability of the inhibition efficiency, IO_3^- stays stable and it has a good inhibition efficiency 72.72 % after 16 days of immersion time in aerated 0.5 M NaCl solution. The molecular modelling as well as quantum chemical simulation precisely the calculation of the both energies. It is found that the E_{HOMO} is located on the Oxygen atoms which indicate that the preferred active sites for an electronic attack and the favorite sites for interactions with the metal surface are located within the region around the Oxygens in the iodate IO_3^-. Which confirm that the iodate molecule adsorbed on the Cu (110) surface.

References

[1] A.H. Jafari, S.M. Hosseini, E. Jamalizadeh, Electrochimica Acta. 55 (2010) 9004-9009.
[2] S. Hong, W. Chen, H.Q. Luo, N.B. Li, Corrosion Sci. 57 (2010) 270-278.
[3] V. Annibaldi, A.D. Rooney, B.C. Breslin, Corrosion Sci. 59 (2012) 179-185.
[4] L. Nüñez, E. Reguera, F. Corvo, R. Gonzãlez, C. Vazquez, Corrosion Sci. 47 (2005) 464-481.
[5] E.M. Sherif, R.M. Erasmus, J.D. Comins, J. Colloid Interface Sci. 309 (2007) 470-477.
[6] B. Hammouti, A. Dafali, R. Touzani, M. Bouachrine, J. Saudi Chemical Soc. 16 (2012) 413-418.
[7] D.Q. Zhang, H. Wu, L.X. Gao, Materials Chemistry and Physics 133 (2012) 981-986.
[8] H.P. Hack, H.W. Pickering, J. Electrochem. Soc. 138 (1991) 690-695.
[9] A.V. Benedetti, P.T.A. Sumodjo, K. Nobe, P.L. Cabot, W.G. Proud, Electrochimica Acta. 40 (1995) 2657.
[10] G. Zhou, H. Shao, B.H. Loo, J. Electroanal. Chem. 421 (1997) 129.
[11] R. Walker, Benzotriazole as a Corrosion Inhibitor for Immersed Copper, Corrosion 29(1973) 290-296.
[12] V. Brusic, M.A. Frisch, B.N. Eldridge, F.P. Novak, F.B. Kaufman, B.M. Rush, G.S. Frankel, J. Electrochem. Soc. 138 (1991) 3483.
[13] D. Tromans, R. Sun, J. Electrochem. Soc. 138 (1991) 3235.
[14] M.M. Antonijevic, M.B. Petrovic, Int. J. Electrochem. Sci. 3 (2008) 1.
[15] C.D.S. Tuck, C.A. Powell, J. Nuttall, Shereir's Corrosion, Vol. 3 (2010) 1937-1973.
[16] T. Attar, L. Larabi, Y. Harek, Hindawi P.C. Advances in Chem. (2014) 1-5.
[17] Luo Q. Langmuir 2000; 16: 5154-8.
[18] K.H. Wall, I. Davies, J. Appl. Chem. 15 (2007) 389-392.
[19] G.W. Poling, , Corrosion Sci. 10 (1970) 359-370.
[20] J. Bariga, B. Coto, B. Fernandez, Tribol. Int. 40 (2007) 960-966.
[21] K.F. Khaled, J. Solid Stat. Electrochem. 13 (2009) 1743.
[22] H.H. Strehblow, B. Titze, Electrochimca Acta. 25 (1980) 839-850.
[23] T. Hashemi, C.A. Hogarth, Electrochimca Acta. 33 (1988) 1123-1127.
[24] D.J. Gardiner, A.C. Gorvin, C. Gutteridge, A.R.W. Jackson, E.S. Raper, , Corrosion Sci. 25 (1985) 1019-1027.
[25] M. Scendo, Corrosion Sci. 47 (2005) 1738-1749.
[26] M. Schlesinger, Modern Aspect of Electrochemistry No. 43 Modeling & Numerical Simulations, 2009.
[27] M.M. Amin, Weight loss, Polarization, J. Appl. Electrochem. 36 (2006) 215-216.
[28] B.V. Appa Rao, M.D. Yakub Iqbal, B. Sreedhar, Acta. 55 (2010) 620-631.
[29] X. Wu, H. Ma, S. Chem, Z. Xu, A. Sui, Electrochem. Soc. 146 (1999) 1847-1853.
[30] E.M. Sherif, S.M. Park, Electrochimica Acta. 51 (2006) 4655-4673.
[31] E.M. Sherif, A.A. Almajid, J. Appl. Electrochem. 40 (2010) 1555-1562.
[32] Q.Q. Liao, Z.W. Yue, Z.H. Wang, Z.H. Li, H.H. Ge, Y.J. Li, Corrosion Science,53 (2011) 1999-2005.
[33] T. Koopmans, Physica. 1 (1934) 104-113.
[34] P. Atkins, J. De Paula, ATKINS' Physical Chemistry, 2006.
[35] H. Chermette, J. Comp. Chem. 20 (1999) 129-154.
[36] R.G. Parr, R.G. Pearson, Principle of Maximum Hardness, J. Am. Chem. Soc. 105 (1991) 7512-7516.
[37] W. Yang, R. G. Parr, Proc. Natl, Acad. Sci. USA 82 (1985) 6723-6726.
[38] R.G. Parr, L. Sventpaly, S. Liu, Electrophilicity Index, J. Am. Chem. Soc. 121 (1999) 1922-1824.
[39] R.G. Pearson, Hard and Soft Acids and Bases, J. Am. Chem. Soc. 85 (1963) 3533-3539.
[40] I. Lukovits, E. Kálmán, F. Zucchi, Corrosion 57 (2001) 3-8.
[41] N.A. Al-Mubarak, K.F. Khaled, M.N.H. Hamed, K.M. Abdel-Azim, N.S. Abdelshafi, Arab. J. Chem. 3 (2010) 233-24